PCCP

PAPER

Quantum effects in the case of $^6Li^+$ and $^7Li^+$ ions evolving in a neutral ^6Li gas at a wide range of temperatures

Cite this: *Phys. Chem. Chem. Phys.*, 2014, **16**, 1875

F. Bouchelaghem[a] and M. Bouledroua*[b]

Received 26th July 2013,
Accepted 29th October 2013

DOI: 10.1039/c3cp53144a

www.rsc.org/pccp

This work deals with the quantum-mechanical calculation of the temperature-dependent mobility of ionic lithium atoms diffusing in their parent gas. The computation of the quantal phase shifts in connection with the gerade and ungerade potential-energy curves, through which Li^+ approaches Li(2s), leads to the computation of the charge-transfer and diffusion cross sections. The behavior of the coefficients of diffusion and mobility with temperature is also examined. Throughout this work, the isotopic effects in the $^6Li^+$–^6Li and $^7Li^+$–^6Li collisions are emphasized.

I. Introduction

Elastic collisions among charged and uncharged atoms have been for decades a trusted source of information on interatomic potentials. Besides, these potentials are required in order to scrutinize the physical mechanisms occurring within gaseous systems and to explore their thermophysical properties and transport coefficients, such as diffusion and mobility.[1] The field became recently of interest to a number of research communities: cold and ultracold chemistry;[2–5] edge and divertor plasmas;[6,7] and ion-mobility spectrometry,[8,9] to just name a few. Hydrogen isotopes and rare-gas and alkali-metal atomic and ionic species have been the main candidates for the theoretical and experimental investigations of like and unlike gases.

In this paper, we present a quantum-mechanical analysis of the elastic and charge-transfer cross sections of lithium system for low and intermediate energies in the range 10^{-13}–10^{-2} a.u. by considering the isotopic and symmetry effects which should be of importance at low energies. The Li_2^+ interaction potentials are constructed upon the published *ab initio* data. These potentials are used to solve the radial wave equation and to determine the quantal phase shifts needed in the computation of the elastic and charge-transfer cross sections. Then, within the so-called Chapman–Enskog model, the thermophysical coefficients and temperature variation laws are examined.

Unless otherwise stated, atomic units (a.u.) are used throughout this paper; in particular, energies are in Hartrees (E_h), distances in Bohrs (a_0), and $\hbar = 1$. The lithium masses involved in the present work are from NIST;[10] they are listed in Table 1.

Table 1 Lithium atomic weights as given in NIST.[10] Numbers in parentheses indicate the uncertainty

Standard Li	^{7}Li	^{6}Li
6.941(2)	7.016 004 55(8)	6.015 122 795(16)

II. Theory

The transport theory of ions in atomic or molecular gases defines the weak-field mobility K at temperature T as[11,12]

$$K = \frac{eD}{k_B T} \quad (1)$$

where e is the ionic charge, k_B is the Boltzmann's constant, and $D = D(T)$ is the temperature-dependent coefficient of diffusion. Usually, to facilitate the comparison of data, the mobility of ions is given as the reduced mobility

$$K_0 = \frac{P}{760}\frac{273.15}{T}K \quad (2)$$

with the gas pressure P being in Torr and T in Kelvin. The diffusion coefficient D is determined with the Chapman–Enskog model for binary systems which considers low-density ions of density n_1 diffusing in a neutral gas of density n_2.[12] If μ denotes the reduced mass of the colliding ion-neutral species, the diffusion coefficient is

$$D(T) = \frac{3k_B T}{16\mu(n_1+n_2)}\frac{1+\varepsilon_0}{\Omega^{(1,1)}(T)}, \quad (3)$$

[a] *Physics Department, Badji Mokhtar University, B.P. 12, Annaba 23000, Algeria*
[b] *Laboratoire de Physique des Rayonnements, Badji Mokhtar University, B.P. 12, Annaba 23000, Algeria. E-mail: boulmoncef@netscape.net*

where $\Omega^{(1,1)}$ is the diffusion collision integral which can be deduced from the more general formula

$$\Omega^{(p,q)}(T) = \sqrt{\frac{k_B T}{2\pi\mu}} \int_0^\infty Q_p(x) x^{2q+3} \exp(-x^2) \mathrm{d}x. \quad (4)$$

In these expressions, $p \geq 1$ and $q \geq 1$ are two integers and the parameter $x^2 = E/k_B T$ is the dimensionless reduced inverse temperature for a given relative energy E. The quantum-mechanical cross section $Q_{p=1}$ effective in diffusion is defined by the summation over the orbital angular momentum l as[12,13]

$$Q_1(E) = \frac{4\pi}{k^2} \sum_{l=0}^{\infty} (l+1) \sin^2(\eta_{l+1} - \eta_l), \quad (5)$$

where $k = \sqrt{2\mu E}$ is the wave number. For the case of dilute gases, that is to say $n_1 \ll n_2$, the correction factor ε_0 in eqn (3) is expressed in Chapman and Cowling[14] as

$$\varepsilon_0 = \frac{5(A-1)^2}{5 - 4B + 8C(M_2/M_1) + 6(M_2/M_1)^2}, \quad (6)$$

where M_1 is the mass of the atomic species diffusing in the buffer gas made of the atomic species of mass M_2. The parameters A, B, and C are the ratios

$$A = \frac{2\Omega^{(1,2)}}{5\Omega^{(1,1)}} \quad (7)$$

$$B = \frac{5\Omega^{(1,2)} - \Omega^{(1,3)}}{5\Omega^{(1,1)}} \quad (8)$$

$$C = \frac{\Omega^{(2,2)}}{5\Omega^{(1,1)}}. \quad (9)$$

In this eqn (9), the viscosity collision integral $\Omega^{(2,2)}$ is calculated from the viscosity cross section $Q_{p=2}$ which is defined by the summation[13]

$$Q_2(E) = \frac{4\pi}{k^2} \sum_{l=0}^{\infty} \frac{(l+1)(l+2)}{2l+3} \sin^2(\eta_{l+2} - \eta_l). \quad (10)$$

For a given energy E, the quantal phase shifts $\eta_l(E)$ in eqn (5) and (10) are computed by imposing the asymptotic behavior

$$\psi_l(R) \sim \sin\left(kR - \frac{l}{2}\pi + \eta_l\right) \quad (11)$$

to the radial wave functions $\psi_l(R)$ of the colliding system. They are solutions of the radial wave equation

$$\left[\frac{\mathrm{d}^2}{\mathrm{d}R^2} + k^2 - 2\mu V(R) - \frac{l(l+1)}{R^2}\right] \psi_l(R) = 0, \quad (12)$$

with $V(R)$ being the ion-neutral interaction potential at the internuclear separation R.

III. Interaction potentials

To solve the above eqn (12) and, hence, determine the phase shifts, the potential $V(R)$ between the lithium ion Li^+ and its neutral ground-state atom Li(2s) has to be known for all distances R. The electronic potential-energy curves through which Li^+ approaches Li, when both species are in their ground states, are either gerade (g) or ungerade (u), namely, $^2\Sigma_g^+$ or $^2\Sigma_u^+$. The two ion-atom potentials should be known in the long, intermediate and short regions for the requisite calculations. We thus adopted the data points in the interval $2 \leq R \leq 50$ produced by Magnier *et al.*[15,16] Both gerade and ungerade data sets are further conveniently extended, for $R \leq 2$, to the Born–Meyer analytical form

$$V(R) \sim \alpha \exp(-\beta R), \quad (13)$$

with α and β being two constants. For the internuclear distances $R \geq 50$, the extension is chosen to be of the form

$$V_{g,u}(R) \sim V_{disp}(R) \mp V_{exch}(R) \quad (14)$$

where the − and + signs are used with the g and u potentials, respectively. The first term $V_{disp}(R)$ is the long-range dispersion potential function defined by the relationship

$$V_{disp}(R) = -\frac{C_4}{R^4} - \frac{C_6}{R^6} - \frac{C_8}{R^8} \quad (15)$$

and the second term $V_{exch}(R)$ represents the exchange energy which becomes very significant when the electronic clouds of the interacting species overlap. We have, in particular, started the above long-range form (15) beyond $R \geq 10$ as required by the Le Roy criterion.[15,17] All the dispersion coefficients, $C_4 = \frac{1}{2}\alpha_d$, $C_6 = \frac{1}{2}\alpha_q$, and $C_8 = \frac{1}{2}\alpha_o$, correlated respectively with the dipole α_d, quadrupole α_q, and octupole α_o polarizabilities of the neutral atom Li(2s), have constant values. Since α_d is determinant in shaping the long-range form of the potentials and fixing the standard mobility, also known as the polarization mobility, in the limit of zero-field strength and zero gas temperature[11]

$$K_{pol} = \frac{13.853}{\sqrt{\mu\alpha_d}}, \quad (16)$$

with μ being in atomic mass units, α_d in Å^3, and K_{pol} in cm^2 V^{-1} s^{-1}, we used here, for both Li_2^+ molecular states, the measured value $\alpha_d = 164.19 \pm 1.10$ of the dipole polarizability recommended by NIST.[10] This α_d is very close to many other polarizabilities that have been generated theoretically or experimentally during the last decade, such as 164.6 of Patil and Tang,[18] 164.0 ± 0.1 of Derevianko *et al.*,[19] and 164.3 ± 1.1 of Jacquey *et al.*[20] A very good compilation of the dipole polarizability data may be found in the very recent review of Mitroy *et al.*[21] We have further adopted the most recent quadrupole $\alpha_q = 1.393 \times 10^3$ and octupole $\alpha_o = 3.871 \times 10^4$ polarizabilities as computed in ref. 18. These results agree quite well with the multipolar polarizabilities $\alpha_q = 1.383 \times 10^3$ and $\alpha_o = 3.680 \times 10^4$ of ref. 22 or $\alpha_q = 1.433 \times 10^3$ and $\alpha_o = 3.915 \times 10^4$ of ref. 23. Moreover, we have also adopted the exchange potential determined by Scott *et al.*[24]

$$V_{exch}(R) = \frac{1}{2}\mathcal{A}^2 R^{2/\gamma - 1} \exp(-\gamma R), \quad (17)$$

with $\gamma = 0.630$ and $\mathcal{A} \simeq 0.815$.[25,26]

The constructed potential-energy curves are displayed in Fig. 1, and the adopted short- and long-range parameters are listed in Table 2. The present g and u curves are also compared with some

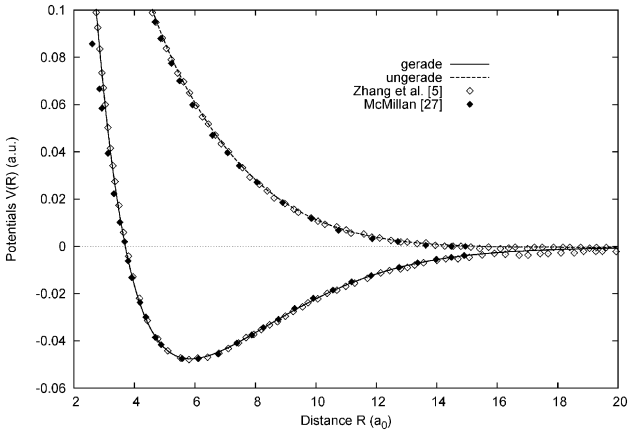

Fig. 1 Potential-energy curves of the gerade and ungerade Li^+–Li electronic states. The curves are compared with published data from Zhang *et al.*[5] and McMillan.[27]

data from Zhang *et al.*,[5] who generated Li_2^+ Born–Oppenheimer potentials, and from McMillan.[27] Quantitatively, the $^2\Sigma_g^+$ potential presents a well depth D_e = 10 447 cm^{-1} corresponding to an equilibrium position R_e = 3.101 Å. These data are comparable with the recent results D_e = 10 475 cm^{-1} and R_e = 3.095 Å of Bouzouita *et al.*[28] and D_e = 10 974 cm^{-1} and R_e = 3.175 Å of Rakshit and Deb.[29] We have also obtained for the very shallow $^2\Sigma_u^+$ potential a well depth D_e = 88.22 cm^{-1} at the equilibrium position R_e = 9.943 Å. Both values are close to D_e = 90 cm^{-1} and R_e = 10.001 Å of Magnier *et al.*[15] and D_e = 88 cm^{-1} and R_e = 9.911 Å of Bouzouita *et al.*[28] The present g and u potential well depths and equilibrium distances are comparable with other works.[30–32]

IV. Elastic cross section

Once we have constructed the potential-energy curves through which an ion and a neutral atom of lithium interact, it is now possible to compute the elastic cross sections relative to both gerade and ungerade states, which are theoretically defined as[13]

$$Q_{el}(E) = \frac{4\pi}{k^2}\sum_{l=0}^{\infty}(2l+1)\sin^2\eta_l. \quad (18)$$

To do so, we should compute primarily the phase shifts $\eta_l = \eta_l(E)$ that are necessary in the determination of the thermophysical features of the Li^+ ions in their ground parent gas Li and their behavior with temperature. In practice, $\eta_l(E)$ are computed for all the energies going from $E_{min} = 10^{-13}$ to $E_{max} = 10^{-2}$ a.u., and the maximum value of the angular momentum l is chosen to be l_{max} = 1000. The quantum-mechanical calculations are carried out up to a certain value $l = l_{sc}$ beyond which the phase shifts are determined semiclassically.[12,13] Assuming for the asymptotic regions that the potentials vary like their most dominant contribution $V(R) \sim -C_4/R^4$, the semiclassical phase shifts are then computed by the simple expression[3]

$$\eta_l(E) = \frac{1}{2}\pi\mu^2 C_4\frac{E}{l^3}. \quad (19)$$

Furthermore, to calculate the Li^+–Li total elastic cross section, it is important to know that, since the collision of both species Li^+ and Li may occur equiprobably *via* the gerade or ungerade potential curve, the average total cross section is[11]

$$Q_{el} = \tfrac{1}{2}(Q_g + Q_u) \quad (20)$$

where Q_g and Q_u are the elastic cross sections for the Li_2^+ gerade and ungerade states. Côté and Dalgarno[3] demonstrated in their work on collisions of ionic sodium Na^+ with neutral Na that the total cross section can be approximated semiclassically by the relationship

$$Q_{el}(E) = \pi\left(\mu\alpha_d^2\right)^{\frac{1}{3}}\left(1+\frac{\pi^2}{16}\right)E^{-\frac{1}{3}}. \quad (21)$$

This expression is gleaned from a procedure fully developed in Mott and Massey[13] and successfully applied to collisions among neutrals and ions with neutrals.[3,33] This equation leads to the numerical result, in a.u.,

$$Q_{el}(E) = 2.642 \times 10^3 E^{-\frac{1}{3}}. \quad (22)$$

On the other hand, it is also convenient to include the possibility of interference between the scattered waves from the symmetrical and antisymmetrical potentials of the molecular ion, as well as the effects of nuclear spin.[11,13] Using the Bose–Einstein statistics, the elastic cross section Q_{el} for $^6Li^+$ ions scattered by ^6Li atoms with identical nuclei of spin s = 1 is given by[11,34]

$$Q_{el} = \frac{s+1}{2s+1}Q^+ + \frac{s}{2s+1}Q^-, \quad (23)$$

where

$$Q^+ = \frac{4\pi}{k^2}\left[\sum_{l\,\mathrm{even}}(2l+1)\sin^2\eta_l^g + \sum_{l\,\mathrm{odd}}(2l+1)\sin^2\eta_l^u\right] \quad (24)$$

and

$$Q^- = \frac{4\pi}{k^2}\left[\sum_{l\,\mathrm{odd}}(2l+1)\sin^2\eta_l^g + \sum_{l\,\mathrm{even}}(2l+1)\sin^2\eta_l^u\right]. \quad (25)$$

Fig. 2 reports the energy dependence of the $^2\Sigma_g^+$ and $^2\Sigma_u^+$ elastic cross sections over a wide range of collisional energies. These cross sections are compared with the very recent data generated by Rakshit and Deb,[29] and the fit given in eqn (22) is also presented. A nice agreement with our calculations is mainly obtained with the u state. Fig. 3 displays the variation with energy of the average cross sections Q_{el} in the case of $^6Li^+$ and $^7Li^+$ ions diffusing in a neutral gas made of neutral ^6Li. We have also presented in the same Fig. 3 the results obtained by Zhang *et al.*[5] for the $^6Li^+$–^6Li system. The graphs show in particular the importance of the isotopic effects at low

Table 2 Short- and long-range parameters of the Li_2^+ potentials. All data are in a.u.

	Short-range		Long-range		
Molecular state	α	β	C_4	C_6	C_8
$^2\Sigma_g^+$	3.354	1.289	82.095	696.50	19.355×10^3
$^2\Sigma_u^+$	2.163	0.899			

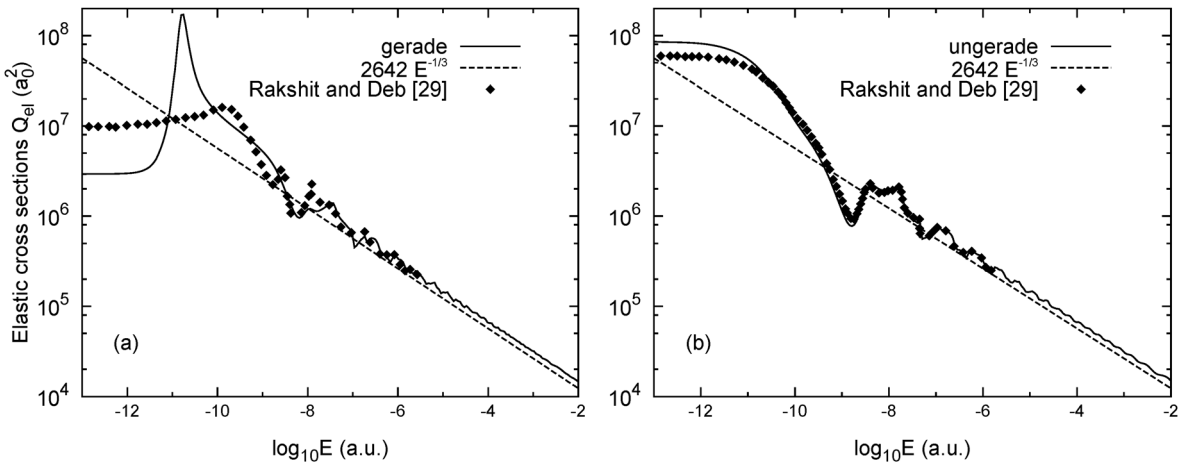

Fig. 2 Elastic g and u scattering cross sections $Q_{el}(E)$ for Li^+ ions scattered by atomic Li. The results are compared with values from Rakshit and Deb.[29] Dashed lines represent the semiclassical cross sections given in eqn (21).

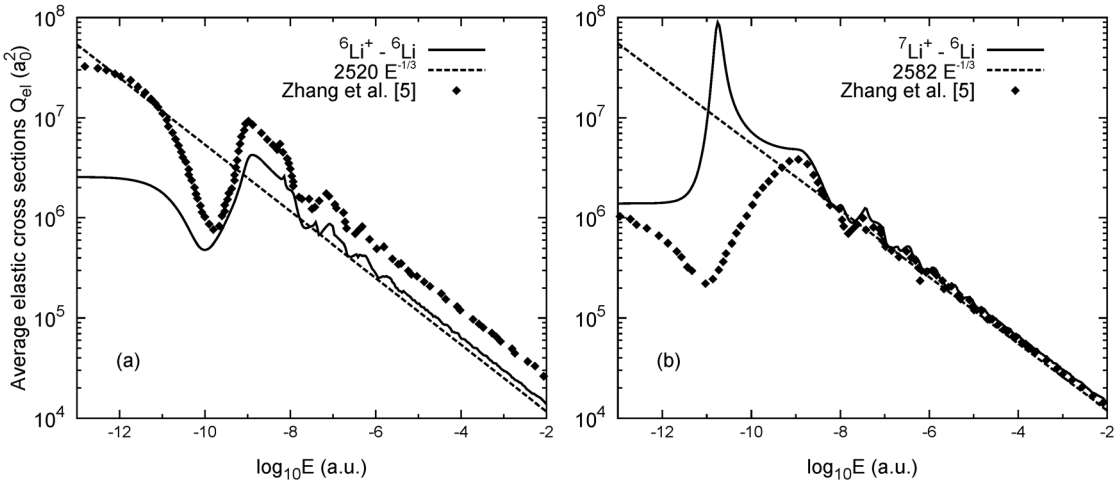

Fig. 3 Average elastic cross sections for both isotopes $^6Li^+$–^6Li and $^7Li^+$–^6Li. The results are compared with data from Zhang *et al.*[5]

collisional energies. Beyond the energy $E \approx 10^{-6}$ a.u., the elastic cross sections of both systems become almost similar, which demonstrates the collapse of the effects of isotopy. It is worth mentioning that the higher-energy elastic cross sections fit the expression $Q_{el}(E) = C_{el}E^{-1/3}$, where $C_{el} = 2.520 \times 10^3$ and $C_{el} = 2.582 \times 10^3$ for the isotopic systems $^6Li^+$–^6Li and $^7Li^+$–^6Li, respectively.

V. Results and discussion

In this section, we shall examine with some theoretical details the thermophysical properties of ionic lithium evolving in a lithium atomic gas and will calculate and analyze the coefficients of diffusion and mobility.

A. Charge transfer

During the collision of an ion with a neutral parent-gas atom, an electron can be transferred from the neutral atom to the ion without affecting the internal energy of the colliding particles. In this case, the cross section for charge transfer is theoretically defined as[11]

$$Q_{ch} = \frac{\pi}{k^2}\sum_{l=0}^{\infty}(2l+1)\sin^2\left(\eta_l^g - \eta_l^u\right). \quad (26)$$

At higher energies, a linear relationship between the square root of the integral cross section for charge transfer and the logarithm of the collision energy[11,34]

$$Q_{ch} = (a\ln E - b)^2 \quad (27)$$

is often a reasonable assumption. If E is expressed in eV, a = 1.77 and b = 27.5 are constant parameters which depend on the collision system under consideration. These two parameters are very close to a = 1.61 and b = 27.8 of Zhang *et al.*[5]

Using the theoretical methods described above, our calculations could output the charge-transfer cross sections $Q_{ch} = 27.1 \times 10^{-15}$ cm^2 at energy E = 0.1 eV and $Q_{ch} = 21.4 \times 10^{-15}$ cm^2 at energy E = 1 eV. For the same energies, the analytical relationship (27) leads to the values 27.9×10^{-15} cm^2 and 21.2×10^{-15} cm^2. All these data agree quite well with the values 26×10^{-15} cm^2 and 22×10^{-15}

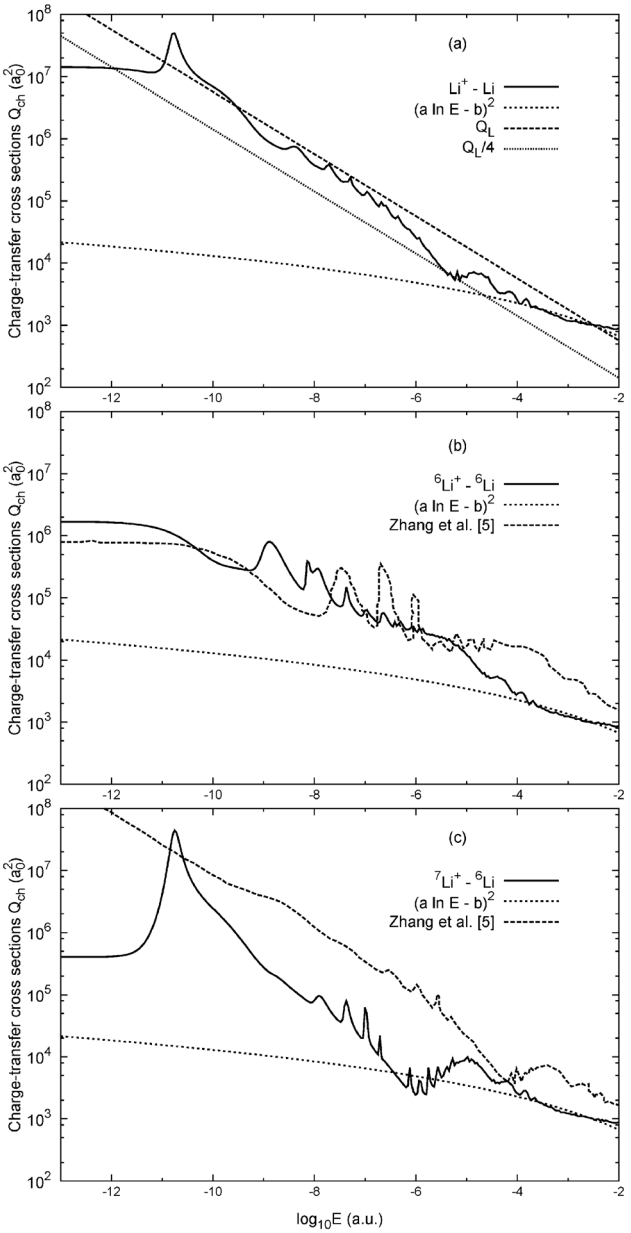

Fig. 4 Li_2^+ charge-transfer cross sections and their behavior with energy. The limit at higher energies is given by eqn (27). The classical Langevin cross sections Q_L and $\frac{1}{4}Q_L$ are presented in (a). The charge-transfer cross sections are given in (b) and (c) for both lithium isotopes and contrasted with the data from Zhang *et al.*[5]

cm^2 given in ref. 26. Moreover, we represent in Fig. 4 our results of the resonant charge-transfer cross sections where the above linearity (27) is verified beyond the energy 10^{-3}. As pointed out in ref. 3 for sodium, the cross sections are dominated, here too, below 10^{-3} by the scattering from the attractive $^2\Sigma_g^+$ interaction varying as R^{-4} and small values of the angular momentum. Fig. 4(a) shows the charge-transfer cross sections Q_{ch} which can be approximated by the classical Langevin relationship

$$Q_L = \pi\sqrt{\frac{2\alpha_d}{E}}, \qquad (28)$$

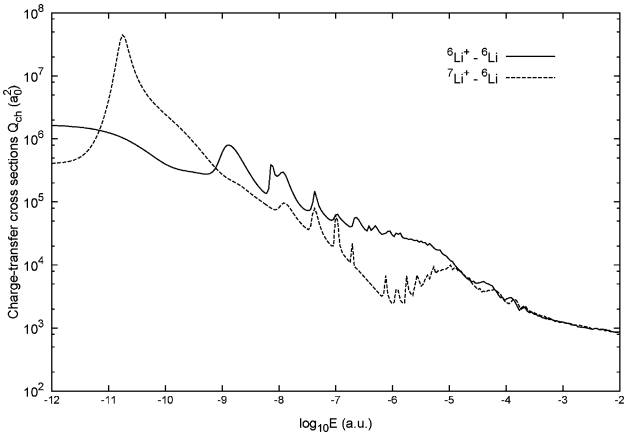

Fig. 5 Charge-transfer cross sections Q_{ch} relative to the $^6Li^+$–^6Li and $^7Li^+$–^6Li collisions.

where the dominant polarization potential has been considered.[3] It essentially shows that the present quantal Q_{ch} results fall, over a wide range of energy, almost entirely within the interval $[\frac{1}{4}Q_L, Q_L]$. Nevertheless, at the thermal energy 1.70×10^{-11}, the present computed value $Q_{ch} = 4.84 \times 10^7 a_0^2$ is significantly higher than the Langevin limit.

In addition, the charge-transfer cross sections for the $^6Li^+$–^6Li and $^7Li^+$–^6Li systems are displayed in Fig. 4(b) and (c) and compared to each other in Fig. 5. One may note from Fig. 5 that the isotopic effects are well pronounced for collisional energies $E \lesssim 10^{-5}$, and both colliding species exhibit orbiting resonances which appear to occur at almost the same energies. Whereas, as the energy increases, the two curves seem to coincide with the form (27). Other calculations, performed by Zhang *et al.*,[5] yielded the data lines illustrated in the same Fig. 4(b) and (c). The agreement between both sets of results is satisfactory, mainly for $^6Li^+$–^6Li.

Finally, the computed low-energy cross sections effective in charge transfer are presented and compared with data from Sinha and Bardsley[35] and Duman and Smirnov[36] in Fig. 6(a). Below $E = 10^{-2}$, we observe small oscillations caused by the interference between each pair of the g and u potential-energy curves. The difference between the gerade and ungerade phase shifts for small partial waves shows significant variations with energy in the region of the potential well, but the curves become practically linear above the energy 10^{-2} (ref. 37). Also, our high-energy cross sections for charge transfer given by eqn (27) are contrasted in Fig. 6(b) with the measurements of Lorents *et al.*,[38] who estimated the experimental error around ±8%, and the theoretical calculations of Firsov.[39] The represented fit in Fig. 6(b) has been realized by these authors with eqn (27).

B. Diffusion and mobility

In a further step, one has to determine first the cross sections effective in diffusion $Q_D = Q_1(E)$ in order to evaluate the temperature-dependent diffusion coefficient $D(T)$ and hence compute the reduced mobility K_0. It is worth mentioning that

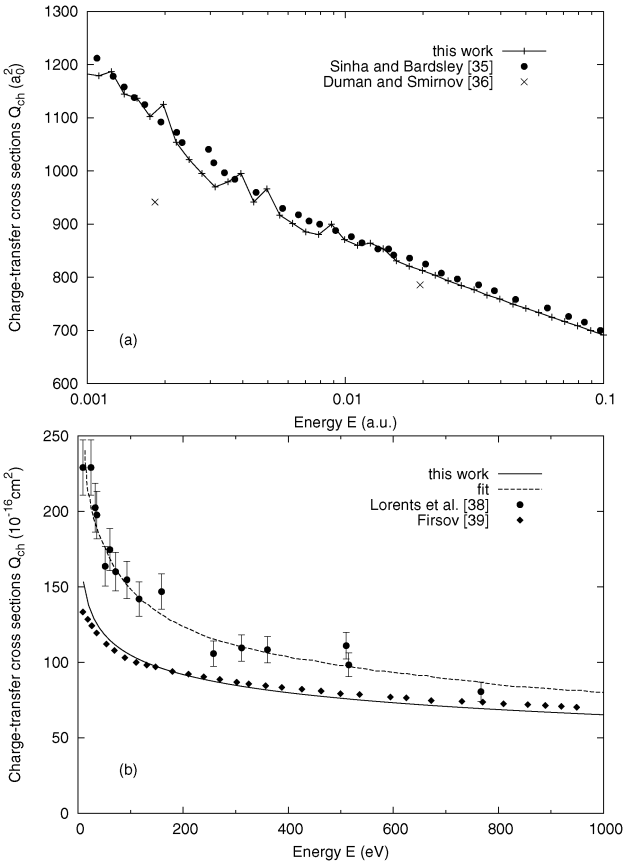

Fig. 6 In (a), charge-transfer cross sections at low energies for standard Li_2^+ compared with data from Sinha and Bardsley[35] and Duman and Smirnov.[36] In (b), high-energy charge-transfer cross sections compared to experimental data from Lorents *et al.*[38] and to the theoretical calculations of Firsov.[39] The fit shown in (b) is also from ref. 38.

we have also attempted to include, for the case of $^6Li^+$ diffusing in ^6Li, the effects of symmetry and spin into the calculations of $D(T)$. The method is very similar to the one used previously with the elastic cross section and eqn (23)–(25) should be adapted to this problem.[34]

Table 3 Temperature dependence of the diffusion coefficient $D(T)$ and correction factor ε_0. Numbers in square brackets are powers of 10

	Li^+ in Li		$^6Li^+$ in ^6Li		$^7Li^+$ in ^6Li	
Temperature T/K	D/cm^2 s^{-1}	ε_0	D/cm^2 s^{-1}	ε_0	D/cm^2 s^{-1}	ε_0
1	1.44[−4]	0.083	1.21[−4]	0.070	1.51[−4]	0.103
50	8.01[−3]	0.093	6.35[−3]	0.079	8.39[−3]	0.115
100	1.69[−2]	0.097	1.18[−2]	0.070	1.77[−2]	0.120
200	3.37[−2]	0.090	2.03[−2]	0.058	3.53[−2]	0.110
300	4.90[−2]	0.083	2.72[−2]	0.052	5.12[−2]	0.101
400	6.41[−2]	0.081	3.36[−2]	0.051	6.69[−2]	0.099
600	1.00[−1]	0.093	4.87[−2]	0.067	1.03[−1]	0.113
800	1.50[−1]	0.119	7.05[−2]	0.098	1.55[−1]	0.114
1000	2.20[−1]	0.148	1.00[−1]	0.132	2.26[−1]	0.180
1500	5.13[−1]	0.213	2.27[−1]	0.207	5.20[−1]	0.259

The obtained diffusion cross sections are displayed in Fig. 7(a) and (b). The first plot represents for standard lithium the variation of Q_D with energy. As predicted in ref. 11 and 34, the calculations show that the diffusion cross sections are at most twice as large as the charge-transfer cross sections, *i.e.*, $Q_D(E) \approx 2Q_{ch}(E)$. On the other hand, Fig. 7(b) illustrates the behavior of Q_D for the cases $^6Li^+$ diffusing in ^6Li and $^7Li^+$ in ^6Li. The isotopic effects are noticeable for energies under 10^{-7}.

We list in Table 3 our theoretical values of $D(T)$ at some temperatures for all the cases dealt with in this work. In particular, the present calculations yield, for $^6Li^+$ diffusing in ^6Li, the values 0.027 and 0.070 cm^2 s^{-1} of the diffusion coefficients at 300 and 800 K, respectively. These data are closely comparable with 0.027 and 0.051 cm^2 s^{-1} of Smirnov.[40] Both values of the diffusion coefficients lead to the same result of the $^6Li_2^+$ reduced mobility K_0, namely, 1.05 cm^2 V^{-1} s^{-1}. Again, they compare well with 1.10 and 0.74 cm^2 V^{-1} s^{-1} cited in ref. 40. The correction factor ε_0, appearing in eqn (3) and (6), is also listed in Table 3 and is displayed as a function of temperature in Fig. 8(a). It emerges from this graph that, apart from a few oscillations observed between 1 K and 500 K around $\varepsilon_0 \sim 8 \times 10^{-2}$, the correction factor increases remarkably beyond 500 K, which should, consequently, have an impact on the variation law of the diffusion coefficient and thus on the reduced mobility.

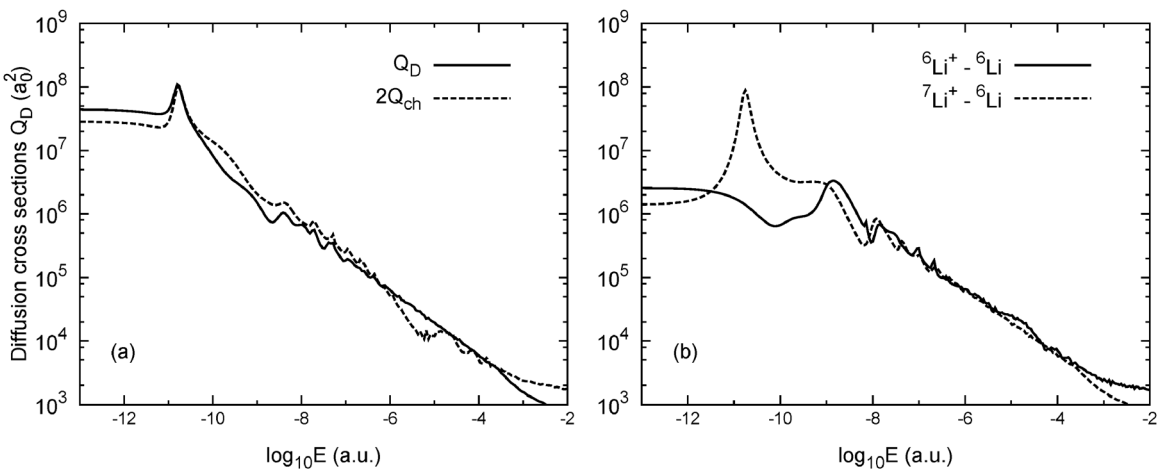

Fig. 7 Diffusion cross sections varying with energy. They are in (a) compared with $2Q_{ch}$ and determined for both lithium isotopes in (b).

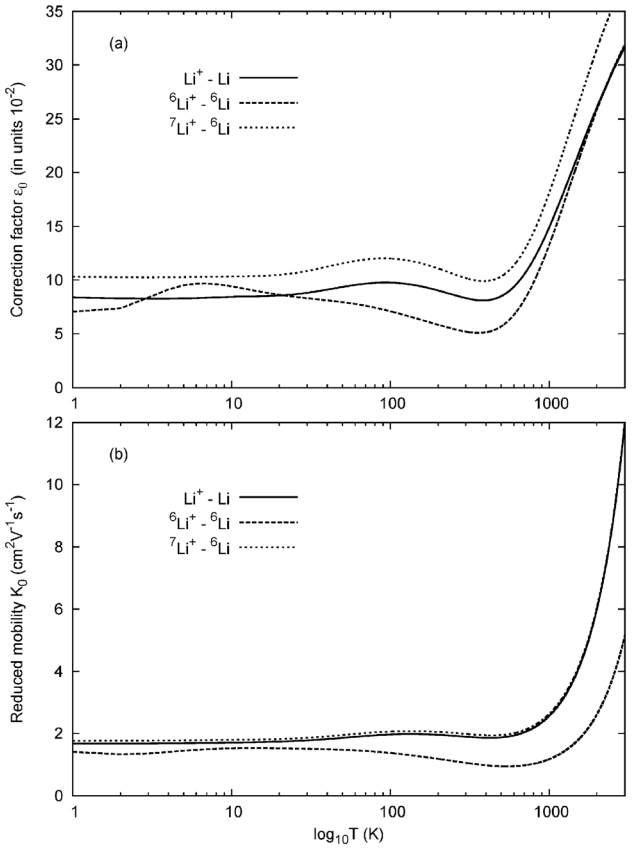

Fig. 8 Correction factor ε_0, in (a), and reduced mobility K_0, in (b), varying with temperature. The curves are given for all the isotopic cases treated in this work.

We have further computed, over a wide range of temperatures, the reduced mobility of Li^+ ions moving in an atomic gas composed of ground lithium. Fig. 8(b) shows the temperature dependence of our calculated mobilities K_0 at gas pressure $P = 760$ Torr. As seen from this Figure, for the standard Li^+ in Li, $^6Li^+$ in ^6Li, and $^7Li^+$ in ^6Li systems, the reduced mobilities tend to the low-temperature values 1.675, 1.372, and 2.063 $cm^2\ V^{-1}\ s^{-1}$, respectively. These values keep approximately constant until the temperature reaches $T \sim 100$ K, beyond which K_0 starts its increase.

VI. Conclusion

In conclusion, we have treated in this work the scattering properties of an ionic lithium evolving in a neutral gas made of atomic lithium. We have in particular analyzed quantum-mechanically the charge-transfer and diffusion cross sections as well as the temperature-dependent transport coefficients, such as the diffusion coefficients and mobility.

Acknowledgements

The authors are very grateful to Dr Monique Aubert-Frécon for providing the Li_2^+ potential data. They also acknowledge the support of the CNEPRU project D01120110036 from the Algerian Ministry of Higher Education and Scientific Research.

References

1 J. B. Hasted, *Physics of Atomic Collisions*, American Elsevier Publishing Company, Inc., New York, 1972.
2 J. Weiner, *Cold and Ultracold Collisions in Quantum Microscopic and Mesoscopic Systems*, Cambrige University Press, New York, 2003.
3 R. Côté and A. Dalgarno, *Phys. Rev. A: At., Mol., Opt. Phys.*, 2000, **62**, 012709.
4 E. Bodo, P. Zhang and A. Dalgarno, *New J. Phys.*, 2008, **10**, 033024.
5 P. Zhang, E. Bodo and A. Dalgarno, *J. Phys. Chem. A*, 2009, **113**, 15085.
6 P. S. Krstić and D. R. Schultz, *At. Plasma-Mater. Interact. Data Fusion*, 1998, **8**, 1.
7 P. S. Krstić and D. R. Schultz, *Phys. Plasmas*, 2009, **16**, 053503.
8 L. A. Viehland and D. E. Goeringer, *J. Phys. B: At., Mol. Opt. Phys.*, 2005, **38**, 3987.
9 C. L. Wilkins and S. Trimpin, *Ion Mobility Spectrometry*, CRC Press, Boca Raton, FL, 2010.
10 http://www.nist.gov.
11 E. A. Mason and E. W. McDaniel, *Transport Properties of Ions in Gases*, Wiley and Sons, Inc., New York, 1988.
12 A. Dalgarno, M. R. C. McDowell and A. Williams, *Philos. Trans. R. Soc. London, Ser. A*, 1958, **250**, 411.
13 N. F. Mott and H. S. W. Massey, *The Theory of Atomic Collisions*, Oxford University Press, Oxford, 1965.
14 S. Chapman and T. G. Cowling, *Mathematical Theory of Non-uniform Gases*, Cambridge University Press, Cambridge, 1939.
15 S. Magnier, S. Rousseau, A. R. Allouche, G. Hadinger and M. Aubert-Frécon, *Chem. Phys.*, 1999, **246**, 57.
16 M. Aubert-Frécon, private communication, 2004.
17 B. Ji, C.-C. Tsai and W. C. Stwalley, *Chem. Phys. Lett.*, 1995, **236**, 242.
18 S. H. Patil and K. T. Tang, *Chem. Phys. Lett.*, 1998, **295**, 152.
19 A. Derevianko, J. F. Babb and A. Dalgarno, *Phys. Rev. A: At., Mol., Opt. Phys.*, 2001, **63**, 052704.
20 M. Jacquey, A. Miffre, G. Trénec, M. Büchner, J. Vigué and A. Cronin, *Phys. Rev. A: At., Mol., Opt. Phys.*, 2008, **78**, 013638.
21 J. Mitroy, M. S. Safronova and C. W. Clark, *J. Phys. B: At., Mol. Opt. Phys.*, 2010, **43**, 202001.
22 J. M. Standard and P. R. Certain, *J. Chem. Phys.*, 1985, **83**, 3002.
23 R. J. Wheatley and W. J. Meath, *Chem. Phys.*, 1994, **179**, 341.
24 T. C. Scott, M. Aubert-Frécon, G. Hadinger, D. Andrae, J. Grotendorst and J. D. Morgan III, *J. Phys. B: At., Mol. Opt. Phys.*, 2004, **37**, 4451.
25 M. Marinescu and A. Dalgarno, *Z. Phys. D: At., Mol. Clusters*, 1996, **36**, 239.

26 B. M. Smirnov, *Phys. Scr.*, 2000, **61**, 595.
27 W. L. McMillan, *Phys. Rev. A: At., Mol., Opt. Phys.*, 1971, **4**, 69.
28 H. Bouzouita, C. Ghanmi and H. Berriche, *THEOCHEM*, 2006, **777**, 75.
29 A. Rakshit and B. Deb, *Phys. Rev. A: At., Mol., Opt. Phys.*, 2011, **83**, 022703.
30 W. Müller and W. Meyer, *J. Chem. Phys.*, 1984, **80**, 3311.
31 I. Schmidt-Mink, M. Müller and W. Meyer, *Chem. Phys.*, 1985, **92**, 263.
32 D. Konowalow and M. E. Rosenkrantz, *Chem. Phys. Lett.*, 1979, **61**, 489.
33 M. Bouledroua, A. Dalgarno and R. Côté, *Phys. Rev. A: At., Mol., Opt. Phys.*, 2001, **65**, 012701.
34 A. Dalgarno, *Philos. Trans. R. Soc. London, Ser. A*, 1958, **250**, 426.
35 S. Sinha and J. N. Bardsley, *Phys. Rev. A: At., Mol., Opt. Phys.*, 1976, **14**, 104.
36 E. L. Duman and B. M. Smirnov, *Sov. Phys. Tech. Phys.*, 1970, **15**, 61.
37 J. A. S. Barata and C. A. N. Conde, *IEEE Trans. Nucl. Sci.*, 2005, **52**, 2889.
38 D. C. Lorents, G. Black and O. Heinz, *Phys. Rev.*, 1965, **137**, A1049.
39 O. B. Firsov, *Zh. Eksp. Teor. Fiz.*, 1951, **21**, 1001.
40 B. M. Smirnov, in *Reviews of Plasma Physics*, ed. V. D. Shafranov, Kluwer Academic/Plenum Publishers, New York, 2003, vol. 23.

